

# TIME SPACE DOMAIN DECOMPOSITION AND REACTIVE TRANSPORT IN POROUS MEDIA

Florian Haeberlein<sup>\*†</sup> and Anthony Michel<sup>\*</sup>

<sup>\*</sup> IFP

1 & 4 avenue de Bois-Préau, BP 311, 92852 Rueil-Malmaison Cedex, France  
e-mail: [firstname.lastname@ifp.fr](mailto:firstname.lastname@ifp.fr), web page: <http://www.ifp.fr/>

<sup>†</sup> Laboratoire Analyse, Géométrie et Applications

Institut Galilée, Université Paris 13, 99 avenue J. B. Clément, 93430 Villetaneuse, France  
e-mail: [haeberlein@math.univ-paris13.fr](mailto:haeberlein@math.univ-paris13.fr), web page: <http://www.math.univ-paris13.fr/laga/>

**Key words:** Convection-diffusion-reaction equations, domain-decomposition

**Summary.** In this paper we present some results concerning the application of time-space domain decomposition methods for reactive transport problems. One of the main objectives of our study is to design local time stepping strategies in order to concentrate numerical efforts on the most reactive part of the domain. This work is a part of the French ANR SHPCO2 project concerning high performance simulation of CO<sub>2</sub> geological storage.

## 1 Introduction

In the context of the ANR SHPCO2 project we are interested in the development of new algorithms to improve the performance of reactive transport solvers for CO<sub>2</sub> geological storage. In order to validate the solutions proposed by different teams, we have designed a synthetic test case (cf. Michel, Haeberlein and Trenty in [6]) that is representative for the industrial process but simple enough to be useful in the prototype development stage.

The storage field is a deep saline aquifer with a thickness of about one hundred metres. The flow is permanently controlled by lateral pressure boundary conditions. For the sake of simplicity, we model the disequilibrium due to the injection of large amounts of CO<sub>2</sub> by a locally perturbed initial condition. Those problem characteristics are illustrated in figure 1. The orange circle represents the area of initial perturbation where most of the chemical phenomena will occur. The strong hydrodynamism present in this case results in a strong coupling of transport and chemistry processes that induce numerical difficulties localised in time and space.

We consider a chemical system of twelve species present in four different phases as follows: CO<sub>2</sub>(g) (gaseous), H<sub>2</sub>O, H<sup>+</sup>, OH<sup>-</sup>, Na<sup>+</sup>, Cl<sup>-</sup>, CO<sub>2</sub>(aq), HCO<sub>3</sub><sup>-</sup>, Ca<sup>++</sup>, SiO<sub>2</sub>(aq)

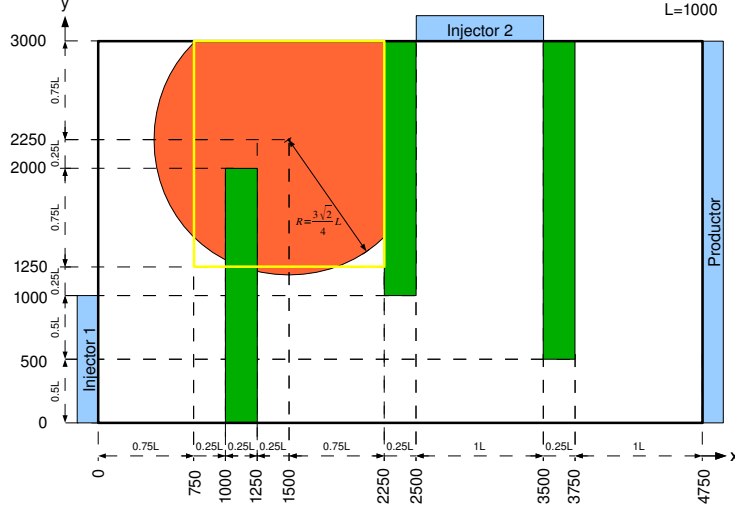
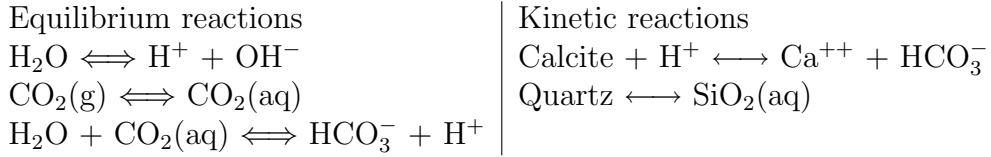


Figure 1: 2D Geometry

(aqueous solution), Calcite (mineral phase) and finally Quartz (mineral phase). Reactions between the species are modelled by the following reactions:



## 2 Reactive Transport Modelling

Having introduced the problem on a chemical and physical level, we formulate now the mathematical modelling. We consider a chemical system containing  $I$  mobile species and  $\bar{I}$  immobile species (distinguished by bars). We numerate such as the first  $I$  species are mobile and the last  $\bar{I}$  species are immobile. A chemical reaction  $j$  is entirely described by its stoichiometric coefficients  $s_{ij}$  for the  $i = 1, \dots, I + \bar{I}$  species. We obtain therefore a stoichiometric matrix  $S$  in which a column correspond to a reaction and a line to a species. Now,  $c_{i=1, \dots, I}$  correspond to the first  $I$  lines of  $S$  and  $\bar{c}_{i=I+1, \dots, I+\bar{I}}$  to the last  $\bar{I}$  lines of  $S$ . Respecting this order, a stoichiometric matrix can be written as follows

$$S := \begin{pmatrix} S_1 \\ -S_2 \end{pmatrix},$$

where  $S_1$  describes the coefficients for the mobile species and  $S_2$  the coefficients for the immobile species. A reactive transport system can be written as

$$\begin{aligned} \partial_t(\phi c) + \mathcal{L}(c) + S_1 R(c, \bar{c}) &= q \\ \partial_t(\phi \bar{c}) + S_2 R(c, \bar{c}) &= 0, \end{aligned} \tag{1}$$

where  $c, \bar{c}$  are the unknown concentrations,  $\phi$  the porosity,  $\mathcal{L}$  a linear transport operator,  $R(c, \bar{c})$  are the reaction rates as functions of the unknown concentrations and  $q$  is a source term.

Following the reduction technique proposed by Kräutle in [5], we can reformulate the problem (1) as follows

$$\begin{aligned}
 \partial_t(\phi\eta) &+ \mathcal{L}(\eta) &= 0 \\
 \partial_t(\phi\bar{\eta}) &&= 0 \\
 \partial_t(\phi\xi_{\text{het}} - \phi\bar{\xi}_{\text{het}}) &+ \mathcal{L}(\xi_{\text{het}}) &= (A_{1,\text{het}} - A_{2,\text{het}})R_{\text{kin}}(c, \bar{c}) \\
 \partial_t(\phi\xi_{\text{kin}}) &+ \mathcal{L}(\xi_{\text{kin}}) &= A_{1,\text{kin}}R_{\text{kin}}(c, \bar{c}) \\
 \partial_t(\phi\bar{\xi}_{\text{kin}}) &&= A_{2,\text{kin}}R_{\text{kin}}(c, \bar{c}) \\
 &&Q(c, \bar{c}) = 0,
 \end{aligned} \tag{2}$$

where  $Q(c, \bar{c})$  describes mass action laws for reformulated equilibrium reactions and  $\eta, \bar{\eta}, \xi_{\text{het}}, \bar{\xi}_{\text{het}}, \xi_{\text{kin}}$  and  $\bar{\xi}_{\text{kin}}$  are linear combinations of the individual concentrations  $c$  and  $\bar{c}$ . System (2) reduces the number of coupled equations and reveals the structure of the interactions between transport and chemistry.

Following the developments of Amir and Kern (cf. [1]) we can now introduce new global variables

$$C := \begin{pmatrix} \eta \\ \xi_{\text{kin}} \\ \xi_{\text{het}} \end{pmatrix}; \quad F := \begin{pmatrix} 0 \\ 0 \\ -\bar{\xi}_{\text{het}} \end{pmatrix}; \quad T := C + F; \quad W := \begin{pmatrix} \bar{\eta} \\ \bar{\xi}_{\text{kin}} \end{pmatrix},$$

where  $T$  is the total part of purely mobile and mixed components,  $C$  its mobile part and  $F$  its fixed part and  $W$  denotes the total concentration of purely immobile components. System (2) can now be reformulated as

$$\partial_t(\phi C) + \partial_t(\phi F) + \mathcal{L}(C) + R_{\text{kin}}^T = 0 \tag{3a}$$

$$\partial_t(\phi W) + R_{\text{kin}}^W = 0 \tag{3b}$$

$$T = C + F \tag{3c}$$

$$F = \Psi(T, W) \tag{3d}$$

$$R_{\text{kin}}^T = \theta(T, W) \tag{3e}$$

$$R_{\text{kin}}^W = \vartheta(T, W), \tag{3f}$$

where  $\theta$  and  $\vartheta$  are functions of  $T$  and  $W$  defining the local kinetic reaction rates.  $\Psi$  denotes a non linear implicit function which represents the result of a reactive flash computation. Following [5] and [1] we solve equations (3a) - (3c) with a global Newton approach with nested local nonlinear problems (3d) - (3f). The derivatives of (3d) - (3f) are obtained by chain rule and implicit function theorem.

### 3 A simplified two species model

We consider a small chemical system of two species denoted by  $u$  and  $v$  where  $u$  is a mobile species and  $v$  is a fixed species. We assume that the chemical system is only governed by the single kinetic reaction  $u \longleftrightarrow v$  characterised by the following reaction rate law

$$R(u, v) := k(x)(v - \Psi(u)).$$

$\Psi(\cdot)$  is in general a non linear sorption isotherm function and  $k(x)$  is a local filter function modelling reactive areas.

In this case, the model reduces to a system of two coupled equations:

$$\begin{aligned} \partial_t(\phi u) + \mathcal{L}(u) - R(u, v) &= f \\ \partial_t(\phi v) + R(u, v) &= 0 \end{aligned} \tag{4}$$

where  $\mathcal{L}(u) := \operatorname{div}(-a\nabla u + bu)$  is a linear transport operator including advection and diffusion-dispersion processes and  $f$  a source term.

### 4 Domain Decomposition

We consider a numerical domain in space  $\mathbb{R}^2$  and in time  $[0, \infty[$ . We define two overlapping subdomains  $\Omega^- = ]-\infty, L] \times \mathbb{R}$ ,  $\Omega^+ = [-L, +\infty[ \times \mathbb{R}$  with  $L \geq 0$  as well as the interfaces  $\Gamma_{12} = \{x = L\} \times \mathbb{R}$ ,  $\Gamma_{21} = \{x = -L\} \times \mathbb{R}$ . We can write a domain decomposition algorithm for system (4)

$$\begin{aligned} \partial_t(\phi u_1^{k+1}) + \operatorname{div}(-a\nabla u_1^{k+1} + bu_1^{k+1}) - k(v_1^{k+1} - \Psi(u_1^{k+1})) &= 0 && \text{in } \Omega^- \times [0, T] \\ \partial_t(\phi v_1^{k+1}) + k(v_1^{k+1} - \Psi(u_1^{k+1})) &= 0 && \text{in } \Omega^- \times [0, T] \\ \mathcal{B}^-(u_1^{k+1}, v_1^{k+1}) &= \mathcal{B}^-(u_2^k, v_2^k) && \text{on } \Gamma_{12} \times [0, T] \end{aligned} \tag{5}$$


---


$$\begin{aligned} \partial_t(\phi u_2^{k+1}) + \operatorname{div}(-a\nabla u_2^{k+1} + bu_2^{k+1}) - k(v_2^{k+1} - \Psi(u_2^{k+1})) &= 0 && \text{in } \Omega^+ \times [0, T] \\ \partial_t(\phi v_2^{k+1}) + k(v_2^{k+1} - \Psi(u_2^{k+1})) &= 0 && \text{in } \Omega^+ \times [0, T] \\ \mathcal{B}^+(u_2^{k+1}, v_2^{k+1}) &= \mathcal{B}^+(u_1^k, v_1^k) && \text{on } \Gamma_{21} \times [0, T] \end{aligned}$$

An initial guess  $(u_1^0, v_1^0)$  and  $(u_2^0, v_2^0)$  has to be furnished in order to start the iteration. Then, the problems can be solved separately in both subdomains  $\Omega_1$  and  $\Omega_2$  providing appropriate coupling operators  $\mathcal{B}^+$  and  $\mathcal{B}^-$  on the interfaces  $\Gamma_{12}$  and  $\Gamma_{21}$ . One might advise that the convergence rate of algorithm (5) is strongly affected by the choice of the coupling operators  $\mathcal{B}^\pm$  on the interfaces.

#### 4.1 Fourier analysis in the linear case

In this section we consider a linear function  $\Psi(u) = cu$  which allows us to develop a rigorous mathematical analysis. Following the ideas proposed by Gander and Halpern in [4] for a scalar reaction-advection-diffusion equation we introduce the transmission

operators

$$\begin{aligned}\mathcal{B}^+(u) &= -a \frac{\partial u}{\partial x} + b_x u + p^+ u \\ \mathcal{B}^-(u) &= a \frac{\partial u}{\partial x} - b_x u + p^- u\end{aligned}\tag{6}$$

where  $p^+$ ,  $p^-$  are real parameters.

Combining (5) and (6) one can express the convergence rate of the algorithm in Fourier space as follows

$$\rho(p^+, p^-, \xi, \tau) = \left| \frac{(b_x + \sigma) - 2p^-}{(-b_x + \sigma) + 2p^-} \cdot \frac{(-b_x + \sigma) - 2p^+}{(b_x + \sigma) + 2p^+} e^{-\frac{2L}{a}\sigma} \right|$$

with  $\sigma := \sqrt{b_x^2 + 4a(\phi i \tau + a\xi^2 + b_y i \xi - \frac{k^2 c}{\phi i \tau + k} + kc)}$  where  $\xi$  is the dual variable of  $y$  and  $\tau$  the dual variable of  $t$ .

In general, we have the property that the larger the overlap  $L$ , the faster the convergence. In practice, the overlap is chosen as  $L \approx \Delta x$  and parameters are set symmetrically  $p = p^+ = p^-$ . In this case, one can prove that the optimal parameter  $p^*$  is solution of the following best approximation problem (cf. [4]):

$$\rho^* = \rho(p^*, \xi^*, \tau^*) = \min_{p>0} \max_{\substack{\tau \in [\frac{\pi}{2T}, \frac{\pi}{\Delta t}], \\ \xi \in [\frac{\pi}{L_y}, \frac{\pi}{\Delta y}]}} \rho(p, \xi, \tau)\tag{7}$$

This problem might be solved numerically but analytical and asymptotic formulae are already available for special cases.

## 5 Numerical results

In the previous section we have developed the domain decomposition theory on a linear function. We are interested in how it is still applicable in a non linear context.

We have developed a numerical 1D prototype that uses an implicit Euler approximation in time and a weighted two-points diffusion and an advection upwind finite volume scheme in space. Numerical solution is obtained by a standard Newton method applied to the global reactive transport system.

### 5.1 Non linear sorption isotherm

We consider an adsorption process that is modelled by a BET isotherm law:

$$\Psi(u) = \frac{Q_s K_L u}{(1 + K_L u - K_S u)(1 - K_S u)}$$

BET theory is a rule for the physical adsorption of gas molecules on a solid surface and serves as the basis for an important analysis technique for the measurement of the specific surface area of a material (cf. [3]). This law is insofar mathematically interesting as it is neither convex nor concave (cf. figure 2).

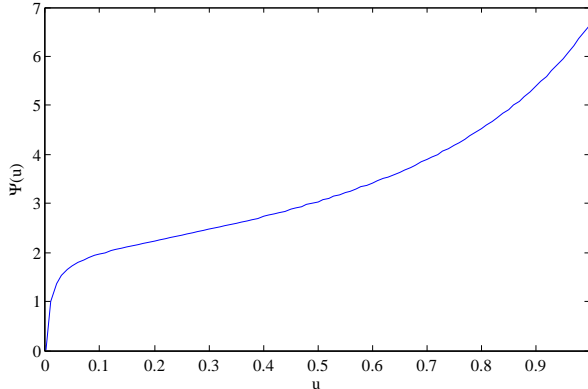


Figure 2: BET Isotherm with  $Q_S = 2$ ,  $K_S = 0.7$ ,  $K_L = 100$

## 5.2 Problem parameters

We inspired our test case from the example of section 1. For numerical simulations, we set the domain to  $\Omega = [-5, 5]$  with  $\Delta x = 0.05$ . Simulation time is  $[0, 1]$ . Physical parameters are  $\phi = 1$ ,  $a = 0.01$ ,  $b = 0.7$ ,  $k = 0.01$ ,  $Q_S = 2$ ,  $K_S = 0.7$ ,  $K_L = 100$ . Initial conditions are set in the following way: considering  $(u_0, v_0) = (0, 0)$  which is an equilibrium state, we perturbate this state for  $u_0$  with an amplitude of 1.0 in a small area (at  $x \in [-4.75, -3.75]$ ) which represents approximately 10% of the whole domain. Boundary conditions for  $u$  are set to Dirichlet with constant values to the equilibrium state  $u_b = u_0$ .

The initially present perturbation of  $u$  turns into an equilibrium state while it is adsorbed from fixed species  $v$ . This creates a strong concentration gradient in  $v$  that has not been present before. As species  $u$  is mobile, the concentration gradient is transported by diffusion and advection. Note that due to the initial perturbation in  $u$  we have created a highly reactive zone. Nevertheless, for the major part of the domain the solution stays nearby an equilibrium state and is more or less stationary.

## 5.3 Monodomain vs. Domain Decomposition solution

In numerical simulations one often limits the time step by controlling the variation of the solution. We also want to do so and fix a time step of  $\Delta t = 0.25$ , i. e. we proceed four time steps in our time window. Note that this choice is not a result of stability condition as we use a fully implicit approach. We are interested in testing the performance of domain decomposition techniques and their capacity to use local time steps. Therefore, we proceed two different numerical simulations and compute approximately the numerical effort in order to compare the competitiveness of our new approach.

First, we calculate a mono-domain approximation using the time step in the entire domain. We set the solution at the previous time step as initial guess for the Newton

iteration and iterate until we have reached a precision of  $10^{-8}$ . In order to reach convergence, (8, 6, 6, 6) iterations are necessary for the four time steps which represents a total effort of  $(8 + 6 + 6 + 6) * 200 = 5200$ .

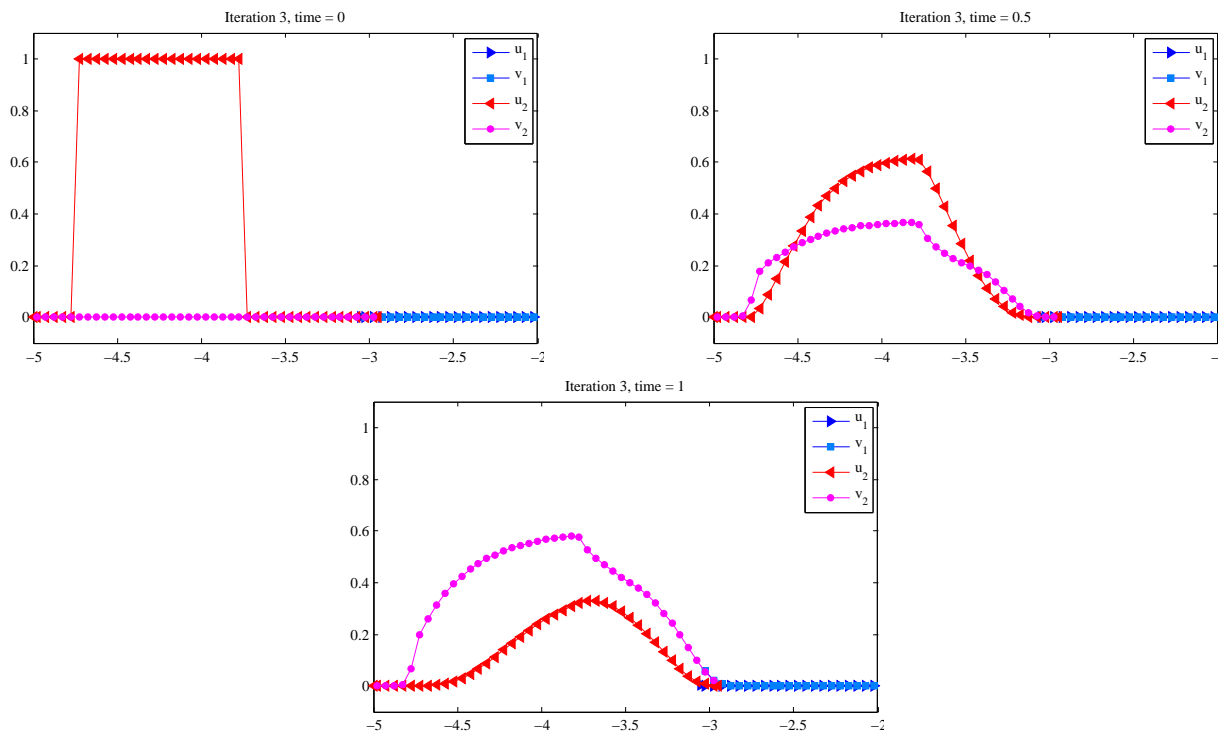


Figure 3: F.l.t.r.: Domain decomposition solution at time  $t = 0, 0.5, 1$

Second, we proceed a domain decomposition method where we set  $\Omega_1 = ]-5, -2.95]$  and  $\Omega_2 = [-3.05, 5]$ , i. e. there is an overlap of size 0.1. In figure 3 we show the solution of the Schwarz algorithm after three iterations in the domain decomposition case, for the initial state  $t = 0.0$ , the intermediate state  $t = 0.5$  and the final time  $t = 1.0$ . Visually, one sees that the initial perturbation touches the interface only at the end of the time window. It is therefore convenient to limit the time step to  $\Delta t_1 = 0.25$  only in the left subdomain while in the right subdomain we can use a coarser time step, say  $\Delta t_2 = 1$ . For the first Schwarz iteration we set the solution of the previous time step as initial guess for the Newton iteration, as we do in the monodomain case. Upon the second Schwarz iterate, we set the solution at the previous Schwarz iteration as initial guess for Newton iterations. For the Schwarz algorithm, we set the initial guess for the interface conditions values to zero and use the parameter for Robin conditions predicted by the theory for linear functions ( $p_{\text{opt}} = 0.7574$ ). Note that this parameter is also the parameter that offers the best numerical performance for the Schwarz algorithm with the non linear function  $\Psi$ . We observe that we need 3 iterations of the Schwarz algorithm in order to reach a precision of  $10^{-6}$ . For the

first Schwarz iteration we need (8, 6, 6, 6) Newton iterations for the left subdomain and (1) Newton iterations in the right subdomain. In the second iterate we need only (1, 1, 1, 1) and (4) iterations, in the third we need (3, 3, 3, 3) and (1) iterations. As a consequence, the total effort is  $((8+6+6+6)+(1+1+1+1)+(3+3+3+3))*40+((1)+(4)+(1))*160 = 2640$ .

To put in a nutshell, by using local time stepping and an optimised Schwarz waveform relaxation algorithm, we reduced the effort for nearly 50 %.

## REFERENCES

- [1] L. AMIR, M. KERN, *Newton-Krylov methods for coupling transport with chemistry in porous media*, CMWR XVI, Copenhagen, June 2006.
- [2] D. BENNEQUIN, M. GANDER AND L. HALPERN, *A Homographic Best Approximation Problem with Application to Optimized Schwarz Waveform Relaxation.*, Math. Comp. 78 (2009), no. 265, 185223.
- [3] S. BRUNAUER, P. H. EMMETT, E. TELLER, *Adsorption of Gases in Multimolecular Layers*, J. Am. Chem. Soc., 60 (2), pp 309–319, 1938.
- [4] M. GANDER AND L. HALPERN., *Optimized Schwarz Waveform Relaxation for Advection Reaction Diffusion Problems.*, SIAM Journal on Numerical Analysis Vol.45, # 2, pp 666–697, 2007.
- [5] S. KRÄUTLE, *General Mutli-Species Reactive Transport Problems in Porous Media: Efficient Numerical Approaches and Existence of Global Solutions*, Habilitation thesis, University of Erlangen-Nuremberg, March 2008.
- [6] A. MICHEL, F. HAEBERLEIN, L. TRENTY, *Cas Tests SHPCO2 n°3 — Test synthétique pour le transport réactif dans le cadre du stockage géologique de CO2*, March 2009.